Composition and structure of apatite formed on organic polymer in simulated body fluid with a high content of carbonate ion

H.-M. KIM*, K. KISHIMOTO, F. MIYAJI, T. KOKUBO
Department of Material Chemistry, Faculty of Engineering, Kyoto University, Sakyo-ku, Kyoto 606-8501, Japan

T. YAO
Department of Fundamental Energy Science, Graduate School of Energy Science Kyoto University, Sakyo-ku, Kyoto 606-8501, Japan

Y. SUETSUGU, J. TANAKA
National Institute for Research in Inorganic Materials, Tsukuba, Ibaraki 305, Japan

T. NAKAMURA
Department of Orthopaedic Surgery, Faculty of Medicine, Kyoto University, Sakyo-ku, Kyoto 606-8506, Japan
E-mail: kim@sung7.kuic.kyoto-u.ac.jp

Apatite layer was formed on polyethyleneterephthalate (PET) substrate by the following biomimetic process. The PET substrate was placed on granular particles of a CaO, SiO_2-based glass in simulated body fluid (SBF) with ion concentrations nearly equal to those of human blood plasma to form apatite nuclei on their surfaces. The apatite nuclei was then grown into a continuous layer by subsequently soaking the substrate in SBF under air or CO_2 atmosphere in which CO_2 partial pressure in the ambient was adjusted to 14.8 kPa to increase the content of carbonate ion to a level nearly equal to that of blood plasma. The increase in the content of carbonate ions in SBF changed the Ca/P atomic ratio of the apatite from 1.51 to 1.63, content of CO_3^{2-} ions from 2.64 to 4.56 wt %, and lattice constants **a** from 94.32 to 94.23 nm and **c** from 68.70 to 68.83 nm, respectively. The Ca/P ratio and lattice constants of the apatite formed in SBF under CO_2 atmosphere were approximately identical to those of bone apatite, i.e. Ca/P atomic ratio 1.65, content of CO_3^{2-} ion 5.80 wt % and lattice constants **a** 94.20 and **c** 68.80 nm. This indicates that an apatite with composition and structure nearly identical to those of bone apatite can be produced in SBF by adjusting its ion concentrations including the content of carbonate ions to be equal to those of blood plasma.

1. Introduction

The present authors have previously proposed a biomimetic process to form a bonelike apatite layer with a desired thickness on any kind and shape of polymer [1–6]: a polymer substrate is placed on granular particles of CaO, SiO_2-based glass soaked in simulated body fluid (SBF) with ion concentrations nearly equal to those of human blood plasma to form a large number of apatite nuclei on its surface, and then the substrate is soaked in another solution highly supersaturated with respect to the apatite, to make the apatite nuclei grow on the substrate *in situ* to form a continuous apatite layer. If the above biomimetic apatite formation could be performed on polymer fabrics to build them up into a three-dimensional structure, such apatite-polymer composites are believed to exhibit mechanical properties analogous to those of natural bone as well as bioactivity, and thus, be truly useful as bone substitutes.

Bioactivity of the apatite-polymer composite prepared by the above biomimetic process is dominated ultimately by the structure and composition of the formed apatite, since the whole surface of the polymer should be covered with the apatite. The best choice is assumed to make the composition and structure of the apatite more identical to bone apatite. The present authors recently revealed that the Ca/P atomic ratio and lattice constants of the apatite vary widely with Ca/P molar ratio, ionic activity products and pH of the solution used for the apatite growth in the second soaking [7–9]. Even the conventional SBF, however, could not provide an apatite with Ca/P atomic

---

* Author to whom all correspondence should be addressed.

0957–4530

ratio and lattice constants equal to those of bone apatite. These results were attributed to the much smaller content of carbonate ions in the fluid than in blood plasma. In the present study, an apatite was formed on an organic polymer in SBF with a high content of carbonate ions. The composition and structure of the apatite were discussed in comparison with those of the apatite formed in SBF under normal conditions and the bone apatite.

2. Materials and methods

2.1. Apatite formation on organic polymer substrate

Organic polymer substrate was polyethyleneterephthalate (PET) $15 \times 10 \times 1\,\mathrm{mm}^3$ in size whose surface was abraded with no. 400 diamond paste, washed with ethanol and dried in air. The PET substrate was subjected to O_2 glow-discharge (GD) treatment in a plasma polymerization system (Model BP-2, SAMCO Ltd, Japan). This GD treatment was previously shown to accelerate apatite nucleation on the substrate [4].

The agent for apatite nucleation was the mother glass of glass-ceramic A-W (glass G), whose nominal composition is MgO 4.6, CaO 44.7, SiO_2 34.0, P_2O_5 16.2, CaF_2 0.5 wt % [10]. Glass G was prepared by conventional melting-quenching technique, and pulverized to be sieved into granular particles 150-300 μmϕ in size.

The solution for apatite nucleation and growth on the substrate was an acellular SBF with pH (7.25) and ion concentrations nearly equal to those of human blood plasma (Table I) [11]. The SBF was prepared by dissolving reagent grade chemicals of NaCl, $NaHCO_3$, KCl, $K_2HPO_4 \cdot 3H_2O$, $MgCl_2 \cdot 6H_2O$, $CaCl_2$ and Na_2SO_4 into distilled water, and buffered at pH 7.25 with tris-hydroxymethylaminomethane ($NH_2C(CH_2\text{-}OH)$) and hydrochloric acid at 36.5 °C.

The PET substrate was placed on 1.5 g particles of glass G in 30 mL of SBF at 36.5 °C for two days to form apatite nuclei on its surface. The substrate was subsequently soaked to make the apatite nuclei grow in 30 mL of SBF at 36.5 °C for six days merely under air atmosphere or under CO_2 atmosphere in which the CO_2 partial pressure was adjusted to 14.8 kPa (Fig. 1). The SBF was renewed every two days during the second soaking period. As shown in Table I, the SBF contains much smaller amounts of HCO_3^{2} ions (4.2 MM) under normal conditions than blood plasma (27.0 MM). Assuming that CO_2 dissolves in water with CO_2/H_2O volume ratio of 0.592 [12], it is estimated that adjusting the CO_2 partial pressure in the ambient to 14.8 kPa could increase the content of HCO_3^{2-} ion in SBF to 27.0 MM by the following equilibria [13]:

$$H_2CO_3 \rightleftarrows HCO_3{}^- + H^+ \qquad K_1 = 4.4 \times 10^{-7} \quad (1)$$

$$HCO_3{}^- \rightleftarrows CO_3{}^{2-} + H^+ \qquad K_2 = 5.6 \times 10^{-11} \quad (2)$$

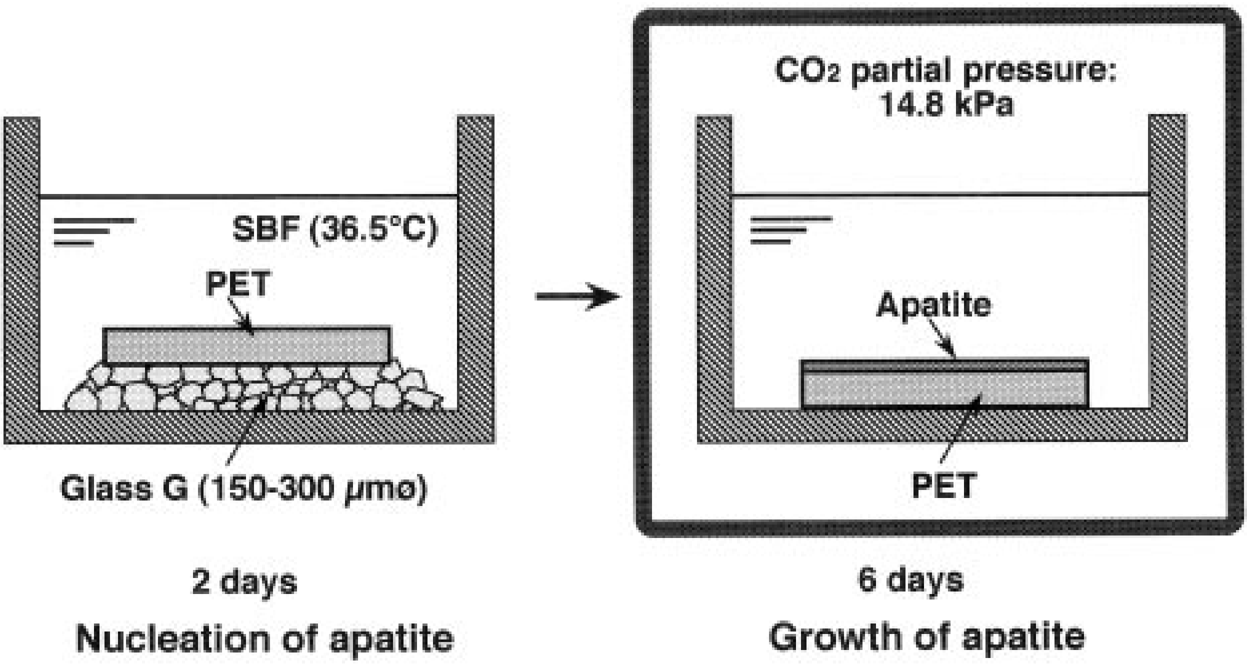

Figure 1 The biomimetic method used in the present study to form an apatite layer on PET substrate in SBF with a high carbonate ion concentration.

TABLE I Ion concentrations of human blood plasma and SBF

	Concentration / MM							
	Na^+	K^+	Mg^{2+}	Ca^{2+}	Cl^-	HCO_3^-	HPO_4^{2-}	SO_4^{2-}
Blood plasma SBF (in air)	142.0	5.0	1.5	2.5	103.0	27.0	1.0	0.5
	142.0	5.0	1.5	2.5	148.8	4.2	1.0	0.5

2.2. Characterization of apatite formed on PET substrates

Apatite formation on the PET substrate was examined by scanning electron microscopy (SEM; S-2500CX, Hitachi Co. Ltd, Japan) and thin-film X-ray diffraction (Tf-xRD; RINt-1400, Rigaku Co., Japan).

Lattice constants **a** and **c** of the apatite were determined by the Rietveld method [14]. XRD data was collected by step-scanning measurement with 0.01° stepping and 10 sec of count time in the 2θ range of 20-60°. The individual *hkl* diffraction peak was expressed by the product of calculated integrated intensity $(I_{calc}(hkl))$ and profile function $(\mathbf{\Omega}_{hkl}(2\theta))$.

$$I_{calc}(hkl) \cdot \mathbf{\Omega}_{hkl}(2\theta) \tag{3}$$

The whole diffraction pattern $(Y_{calc}(2\theta))$ was then given by summing all the peaks and adding background $(Q(2\theta))$.

$$Y_{calc}(2\theta) = \Sigma I_{calc}(hkl) \cdot \mathbf{\Omega}_{hkl}(2\theta) + Q(2\theta) \tag{4}$$

Pseudo-voigt function [15] was used to describe the profile shape. The background was obtained from the diffraction data for the original substrate. The lattice constants included in the profile function as variable parameters and other profile/structure parameters were then refined to minimize the reliability factor (R_{wp}) defined as

$$R_{wp} = \left\{ \frac{\Sigma[Y_{obs}(2\theta_i) - Y_{obs}(2\theta_i)]^2}{\Sigma[Y_{obs}(2\theta_i)]^2} \right\}^{1/2} \tag{5}$$

where $Y_{obs}(2\theta_i)$ is the observed intensity at $2\theta_i$. The Rietveld calculation was performed by using a computer program named RIEVEC [16].

The apatite was also analyzed by Fourier transform infrared (FTIR) absorption spectroscopy (System 2000, Perkin-Elmer Ltd, UK). The apatite was scratched from the substrates, heated at 150 °C for 3 h to remove adsorbed water, mixed with KBr powder at 1 : 100 in weight ratio, and pressed into pellet form to be subjected to FTIR measurement.

In order to analyze the composition of the apatite, the apatite was dissolved in 6M-HCl solution and subjected to inductively coupled plasma (ICP) atomic emission spectroscopy (SPS-1500 VR, Seiko Instruments Inc., Japan).

The content of water and carbonate in the apatite were analyzed by a carbon and water determinator (RC-412, LECO Co., USA). About 50 mg of the apatite was gathered from the substrate, heated at a rate of 3 °C/min. The amounts of CO_2 and H_2O gases released at given temperatures were measured from IR absorption peaks at 670 and 3010-3020 cm^{-1}, respectively.

3. Results

3.1. SEM observation

Fig. 2 shows the SEM photographs of the surfaces of PET substrates after soaking in SBF under air and CO_2 atmospheres. It can be seen from Fig. 2 that dense and uniform layers of deposits are formed on the surface of the substrate in SBF under both conditions.

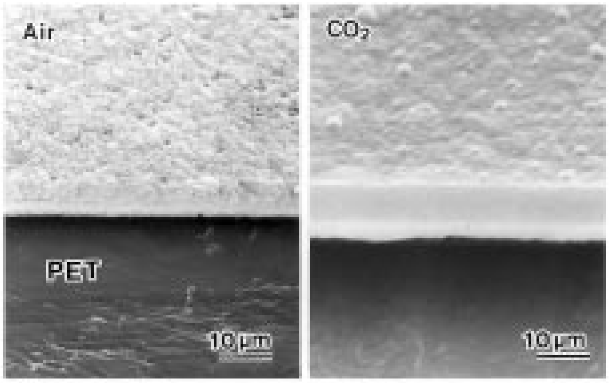

Figure 2 SEM photographs of the surfaces of PET substrates after soaking in SBF under air and CO_2 atmospheres.

3.2. Tf-XRD analysis

Fig. 3 shows the TF-XRD patterns of the surfaces of PET substrates before and after soaking in SBF under air and CO_2 atmospheres. XRD peaks appeared after the soaking, and were all ascribed to a crystalline apatite, indicating that the deposits on the substrates in Fig. 2 are apatite.

Fig. 4 shows the Rietveld refinement plot of the TF-XRD pattern of the apatite formed on PET substrate in SBF under CO_2 atmosphere. The reliability factor calculated by the method described above was 0.0626, which was small enough to provide a good fitting for

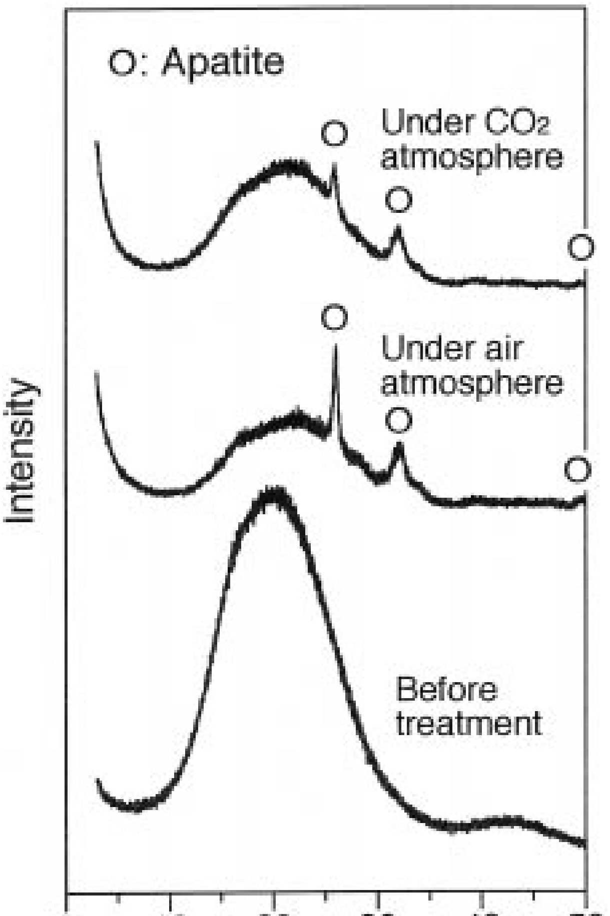

Figure 3 TF-XRD patterns of the surfaces of PET substrates before and after soaking in SBF under air and CO_2 atmospheres.

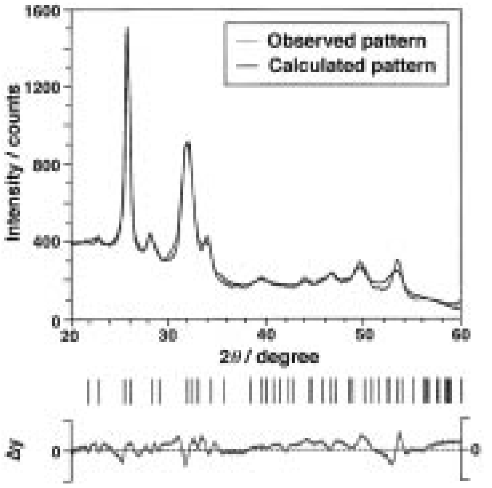

Figure 4 Rietveld refinement plot of the TF-XRD pattern of the apatite formed on PET substrate in SBF under CO_2 atmosphere. The calculated and observed patterns are shown on the top; the positions of calculated Bragg reflections with vertical marks in the middle; a plot of the difference between the observed and the calculated at the bottom.

assuring precision of lattice parameters. The lattice constants **a** and **c** calculated from this result were 94.23 and 68.83 nm, respectively. Those of the apatite formed on the PET substrate under air atmosphere were obtained as **a** = 94.32 and **c** = 68.70 nm by the same method.

3.3. FTIR analysis

Fig. 5 shows the FTIR transmission spectra of the apatite formed on PET substrates in SBF under air and CO_2 atmospheres. Peak assignments were based on the previous reports by Hench [17] and Gee and Deitz [18]. Peaks ascribed to CO_3^{2-} were observed at about 871 and 1450 cm^{-1} besides the main peaks ascribed to the apatite [19, 20]. Peaks ascribed to $P_2O_7^4$ were also observed at about 730 and 1200 cm^{-1}. The $P_2O_7^{4-}$ ions are speculated to be formed by heat treatment of HPO_4^{2-} ions. This indicates that the apatite formed on the substrates contains both the CO_3^{2-} and HPO_4^{2-} ions.

3.4. ICP atomic emission spectroscopy analysis

The Ca/P atomic ratios of the apatite formed on PET substrate in SBF under air and CO_2 atmospheres were measured to be 1.51 and 1.63, respectively. The Mg/Ca and Na/Ca ratios were the same under both conditions, 0.040 and 0.030, respectively.

3.5. Thermal analyzes

Fig. 6 shows the release of CO_2 and H_2O gases from the apatite formed on PET substrate in SBF under CO_2 atmosphere on heating at a rate of 3 °C/min. The total amounts of CO_2 and H_2O gases released from the apatite were calculated to be 3.86 and 15.40 wt %, respectively. The amount of H_2O gas due to absorbed water released at 92 °C was 15.35 wt %. The net content of carbonate ions of the apatite was thus estimated to be 4.56 wt %. The content of carbonate ions of the apatite formed on PET substrate in SBF under air atmosphere was estimated to be 2.64 wt % by the same method.

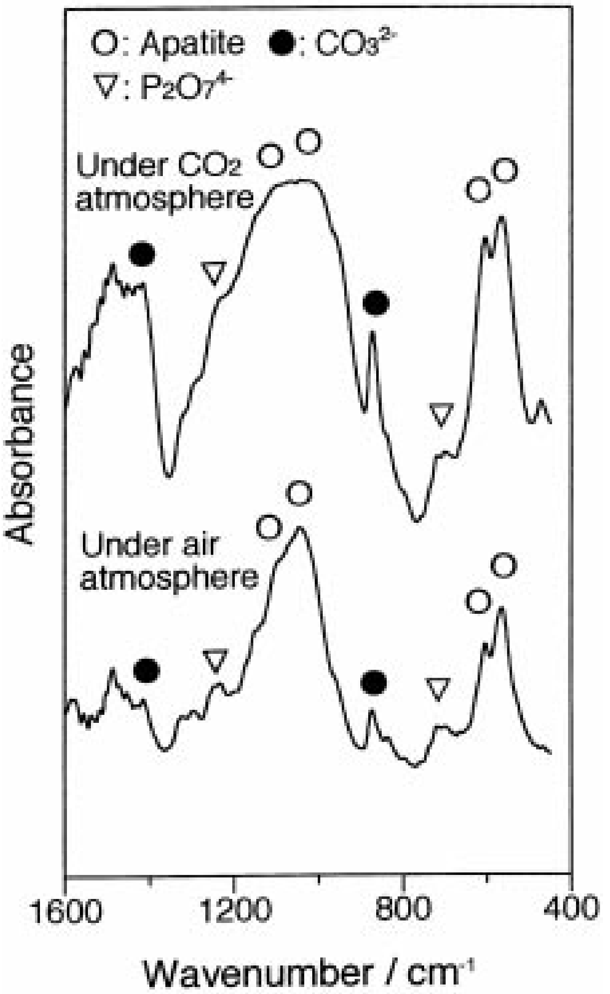

Figure 5 FTIR transmission spectra of the apatite formed on PET substrates in SBF under air and CO_2 atmospheres.

4. Discussion

Table II summarizes the lattice constants and compositions of the apatite formed on the substrate in SBF under air and CO_2 atmospheres, in comparison with those of stoichiometric hydroxyapatite and bone apatite. It is apparent from the above results that the composition and structure of the apatite produced in SBF widely differ due to the content of carbonate ions in the SBF.

It is well known that composition of an apatite deposited in an aqueous solution is largely dependent upon the content of its constituent components in the solution. Although all the other compositions, e.g. Ca/P, Mg/Ca and Na/Ca molar ratio, excepting the content of carbonate ions in SBF, were unchanged under both the conditions, compositional differences were shown clearly for Ca/P atomic ratios as well as the content of CO_3^{2-} ions of the apatite formed in SBF under air and CO_2 atmospheres. Stoichiometric apatite is given by a chemical formula $Ca_{10}(PO_4)_6(OH)_2$ with Ca/P atomic ratio of 1.67. When an apatite is deposited from an aqueous solution, some sites for PO_4^{3-} ions are often

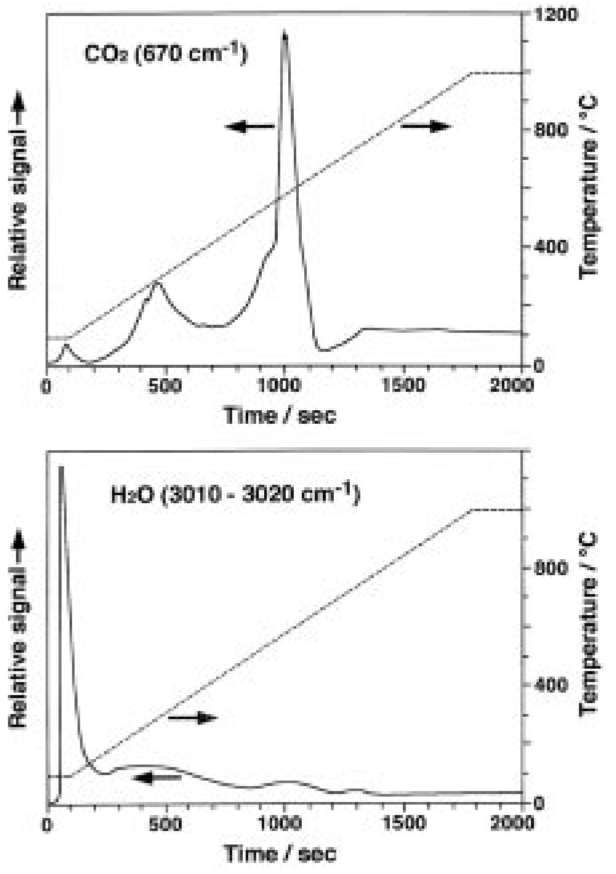

Figure 6 Release of CO_2 and H_2O gases from the apatite formed on PET substrate in SBF under CO_2 atmosphere on heating at a rate of 3 °C/min.

substituted by HPO_4^{2-} and CO_3^{2-} ions. Vacancies are thus produced in the sites for Ca^{2+} for maintaining electrical neutrality. It is clear from Fig. 5 that the apatite formed in SBF also susbtitutes HPO_4^{2-} and CO_3^{2-} ions for PO_4^{3-} sites; IR absorption peaks at 871 and 1450 cm^{-1} and those at 730 and 1200 cm^{-1} are respectively due to the CO_3^{2-} and HPO_4^{2-} ions occupying the PO_4^{3-} sites [19]. One substitution of CO_3^{2-} for PO_4^{3-} results in one P and half Ca deficiencies to give a Ca/P ratio larger than 1.67, while one HPO_4^{2-} for PO_4^{3-} results in only half Ca deficiency to give a Ca/P ratio lower than 1.67. This means that the Ca/P ratio of the apatite could be the larger when more CO_3^{2-} ions occupy PO_4^{3-} sites instead of the HPO_4^{2-}. It is therefore speculated that much larger $CO_3{}^{2-}$ ion concentration in the apatite formed in the SBF under CO_2 atmosphere than under air atmosphere is responsible for the larger Ca/P atomic ratio of the apatite formed in the former condition.

Stoichiometric apatite takes a hexagonal structure and its lattice constants **a** and **c** are 94.20 and 68.80 nm, respectively [21]. Substitution of PO_4^{3-} ions with CO_3^{2-} is known to expand the hexagonal lattice along the *c* axis, since the O-C-O angle is larger than the O-P-O angle [22]. The differences in the lattice constants between the apatite formed in SBF under air and CO_2 atmospheres correspond well to this account. The larger CO_3^{2-} ion concentration in the latter apatite is attributed to the smaller lattice constant a and larger c than those of the former apatite.

It should be noted in Table II that the composition and structure of the apatite formed in SBF under CO_2 atmosphere is fairly similar to those of bone apatite. These results correspond well to our previous prediction that an SBF with ion concentrations, including its carbonate ion content, more identical to the blood plasma will produce the more bone-like apatite.

5. Conclusions

An apatite layer with composition and structure approximately the same as those of bone apatite could be formed on an organic polymer in SBF by increasing its carbonate ion content to a level equal to that of blood plasma. This indicates that an apatite with composition and structure nearly identical to those of bone apatite can be produced in SBF by adjusting its ion concentrations including the carbonate ion content to be equal to those of blood plasma.

References

1. M. TANAHASHI, T. KOKUBO, M. MINODA, T. MIYAMOTO, T. NAKAMURA and T. YAMAMURO, *J. Am. Ceram. Soc.* **77** (1994) 2805.
2. *Idem., J. Appl. Biomater.* **5** (1994) 339.
3. *Idem., J. Mater. Sci.: Mater. Med.* **6** (1995) 319.
4. M. TANAHASHI, T. YAO, T. KOKUBO, M. MINODA, T. MIYAMOTO, T. NAKAMURA and T. YAMAMURO, *J. Biomed. Mater. Res.* **29** (1995) 349.
5. K. HATA and T. KOKUBO, *J. Am. Ceram. Soc.* **78** (1995) 1049.
6. G. J. LIU, F. MIYAJI, T. KOKUBO, H. TAKADAMA, T. NAKAMURA and A. MURAKAMI, *J. Mater. Sci.: Mater. Med.* **9** (1998) 285.
7. F. MIYAJI, K. KISHIMOTO, T. KOKUBO, T. YAO, T. NAKAMURA, Y. SUETSUGU and J. TANAKA, *Biomaterials* (submitted).

TABLE II Lattice constants, Ca/P, Mg/Ca and Na/Ca atomic ratios, and content of $CO_3{}^{2-}$ of the apatite formed on PET substrates in SBF under air and CO_2 atmospheres, in comparison with those of stoichiometric hydroxyapatite and bone apatite

	Lattice constant/nm		Ca/P	Mg/Ca	Na/Ca	$CO_3{}^{2-}$ / wt%
	a	**c**				
Apatite formed in SBF under air	94.32	68.70	1.51	0.040	0.030	2.64
Apatite formed in SBF under CO_3^{2-}	94.23	68.83	1.63	0.040	0.030	4.56
Stoichiometric hydroxyapatite*	94.20	68.80	1.67	–	–	–
Bone apatite⁺	94.19	68.80	1.65	0.016	0.022	5.80

*[21].
⁺[22].

8. H.-M. KIM, K. KISHIMOTO, F. MIYAJI, T. KOKUBO, T. YAO, Y. SUETSUGU, J. TANAKA and T. NAKAMURA, *J. Biomed. Mater. Res.* **46** (1999) 228.
9. H.-M. KIM, K. KISHIMOTO, F. MIYAJI, T. KOKUBO and T. NAKAMURA, *J. Ceram. Soc. Japan.* (submitted).
10. T. KOKUBO, M. SHIGEMATSU and T. YAMAMURO, *J. Mater. Sci.* **21** (1986) 536.
11. T. KOKUBO, H. KUSHITANI and S. SAKKA, *J. Biomed. Mater. Res.* **24** (1990) 721.
12. S. NAGAKURA, H. IGUCHI, H. EAZAWA, S. IWAMURA, F. SATOU and R. KUBO ''Iwanami-rikagaku-ziten,'' 5th Edn (Iwanami-syouten, Tokyo, 1987) p. 975.
13. R. C. WEAST, D. R. LIDE, M. J. ASTEL and W. H. BEYER, ''CRC Handbook of Chemistry and Physics,'' 70th Edn (CRC Press, Boca Raton, FL, 1989) p. d-165.
14. H. M. RIETVELD, *J. Appl. Cryst.* **2** (1969) 65.
15. R. A. YOUNG, ''The Rietveld Method'' (Oxford University Press, London, 1993).
16. T. YAO, ''Report of Grant-in-aid for Scientific Research (No. 02650560) from the Ministry of Education, Science, Sports and Culture'' (Japan, 1992).
17. L. L. HENCH, *J. Am. Ceram. Soc.* **74** (1991) 1487.
18. A. GEE and V. DEITZ, *ibid.* **77** (1955) 2961.
19. C. REY, B. COLLINS, T. GOEHL, I. R. DICKSON and M. J. GLIMCHER, *Calcif. Tissue Int.* **45** (1989) 157.
20. C. Y. KIM, A. E. CLARK and L. L. HENCH, *J. Non-cryst. Solids* **113** (1989) 195.
21. R. A. YOUNG and J. C. ELLIOT, *Archs. Oral. Biol.* **11** (1966) 699.
22. R. Z. LEGEROS and J. P. LEGEROS, in ''An Introduction to Bioceramics'', edited by L.L. Hench and J. Wilson (World Scientific, Singapore, 1993) p. 139.

Received 11 December 1998
and accepted 14 January 1999